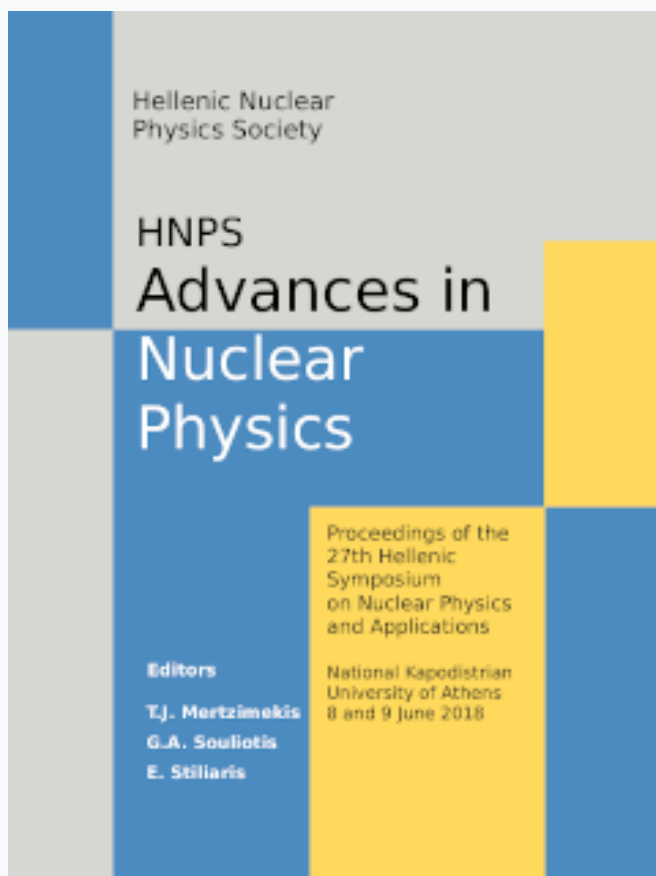


## HNPS Advances in Nuclear Physics

Vol 26 (2018)

HNPS2018



### Nuclear magnetic moment studies of short-lived excited states at the edge of the island of inversion: the IS628 experiment

*A. Khaliel, D. Papaioannou, G. Zagoraios, T. J. Mertzimekis*

doi: [10.12681/hnps.1795](https://doi.org/10.12681/hnps.1795)

#### To cite this article:

Khaliel, A., Papaioannou, D., Zagoraios, G., & Mertzimekis, T. J. (2019). Nuclear magnetic moment studies of short-lived excited states at the edge of the island of inversion: the IS628 experiment. *HNPS Advances in Nuclear Physics*, 26, 44–50. <https://doi.org/10.12681/hnps.1795>

# Nuclear magnetic moment studies of short-lived excited states at the edge of the island of inversion: the IS628 experiment

A. Khaliel\*, D. Papaioannou, G. Zagoraios and T.J. Mertzimekis for the IS628 collaboration

*Department of Physics, University of Athens, Zografou Campus, GR-15784, Athens, Greece*

---

**Abstract** Nuclear  $g$  factors are highly sensitive to the single-particle aspects of the wave function, revealing important information for the nuclear structure along the isotopic chart. The  $sd$  shell has been thoroughly studied, resulting in “universal” shell model Hamiltonians [1] and the development of an M1 operator [2]. However, there is still shortage of precise experimental  $g$  factor data of excited states to consolidate the nuclear structure in this regime.

Recently, the Time Differential Recoil in Vacuum (TDRIV) experimental technique was revamped to be applicable for radioactive beams. TDRIV has been tested successfully and produced high-precision results for the stable  $^{24}\text{Mg}$  nucleus [3]. However, the successful application of the technique relies heavily on calibrations of the de-orientation phenomenon.

A recent experiment using the MINIBALL array at REX/ISOLDE (IS628) has focused on the application of the method with a radioactive  $^{28}\text{Mg}$  beam. The  $g$  factor of the  $^{28}\text{Mg}$  first  $2^+$  excited state can act as an excellent probe of the  $N=16$  shell gap and the  $vd_{3/2}$  singleparticle energy, as well as the possible presence of  $spdf$  admixtures. The particular measurement will be a next step towards a  $g$  factor measurement on  $^{32}\text{Mg}$  in the center of the “island of inversion”, where the  $N=20$  shell closure breaks down enhancing  $1p-1h$  excitations and shape-coexistence.

In this work, the analysis of the spectroscopic data recorded for a  $^{22}\text{Ne}$  beam, which was used for calibrating the experimental method before the actual run on  $^{28}\text{Mg}$  is reported. Preliminary data on the angular distributions for the  $^{22}\text{Ne } 2_1^+ \rightarrow 0^+$  transition will be presented, an important prerequisite before a remeasurement of  $g(^{22}\text{Ne}; 2_1^+)$ .

**Keywords**  $g$  factor,  $^{28}\text{Mg}$ , TDRIV, MINIBALL, island of inversion

---

## INTRODUCTION

Nuclear  $g$  factor measurements can provide us with important information regarding the nuclear wavefunction, due to their extreme sensitivity in the single-particle aspects of the corresponding nuclear state. The nucleus  $^{28}\text{Mg}$  belongs to the  $sd$  shell, which has been thoroughly studied. These studies resulted in new universal Hamiltonians [1] for the  $sd$  shell, as well as an effective M1 operator [2]. However, there is a shortage of  $g$  factor data of excited states in the  $sd$  (and in general), which would stringently constrain the above models.

Experimental studies dedicated to exotic neutron-rich nuclei for about  $N=20$  has shown that unexpected changes occur in their shell-structure. The traditional shell-closures break down, due to the monopole component of the residual interaction of the valence nucleons,

---

\* Corresponding author, email: achalil@phys.uoa.gr

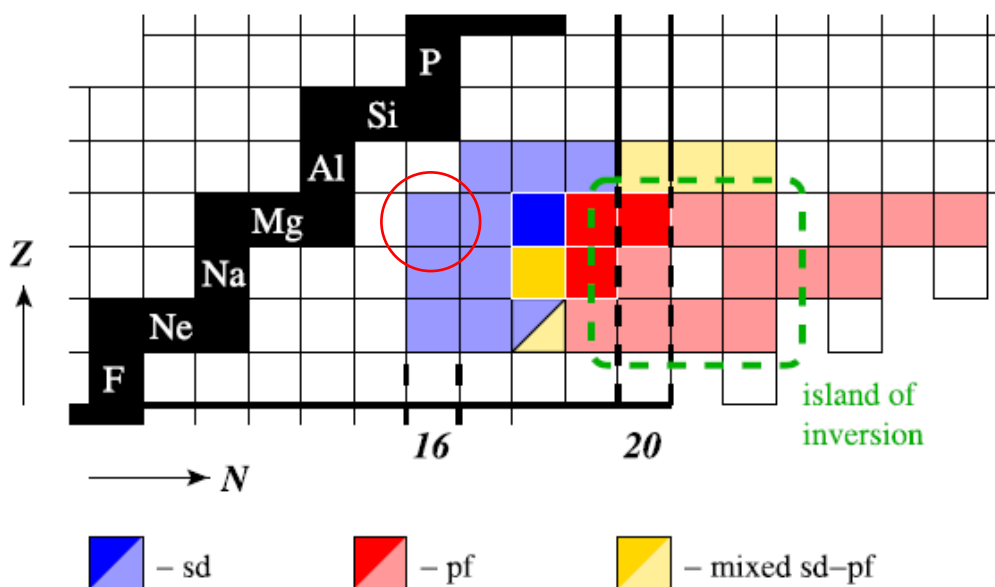


**Figure 1:** Part of the *sd* shell, showing the island of inversion near  $^{32}\text{Mg}$  (green dashed line).  $^{30,31,32}\text{Mg}$  and  $^{29,30}\text{Na}$  have been investigated at REX-ISOLDE by means of safe Coulou and transfer reactions. The transition between normal *sd* ground-state configuration and the intruder *pf* configuration is delineated [4].

resulting in significant shifts of the single-particle energies and the emergence of new shell gaps [4]. Such areas in the nuclear chart are called “islands of inversion” and one of these lies around the nucleus  $^{32}\text{Mg}$ . Part of the *sd* shell near the island of inversion around  $^{32}\text{Mg}$  is shown in Fig. 1. The study of  $^{28}\text{Mg}$ , which is marked with a red circle, will significantly help in defining the boundaries of the island of inversion and also pave the way for a *g* factor measurement of  $^{32}\text{Mg}$ , inside the island of inversion.

## EXPERIMENTAL METHOD

Recently, the traditional Time-Differential Recoil In Vacuum (TDRIV) technique has been modified in order to suit experiments with radioactive beams [5]. This modernized version has been tested with a *stable* beam [3] and provided results which agree with previous measurements, but are significantly more precise. In this way, *g* factors of excited states can now be measured with exceptional precision (~5%). In this work, the technique is used for the first time with a *radioactive* beam.

The  $2_1^+$  state of  $^{28}\text{Mg}$  was populated via Coulomb excitation at a beam energy of 5.5 MeV/u. The  $^{28}\text{Mg}$  beam impinged on a  $^{93}\text{Nb}$  target mounted on a plunger device and placed at the center of the MINIBALL array [6]. The *g* factor can be determined by measuring the precession of the nuclear spin, as H-like ions emerge from the Nb foil. The nuclear spin **I** is aligned by the reaction, while the atomic spin **J** is oriented randomly. The nuclear spin couples with the atomic spin, and together they undergo precession about the total spin **F** = **I** + **J** inside the plunger chamber with a frequency proportional to the *g* factor (Fig. 2).

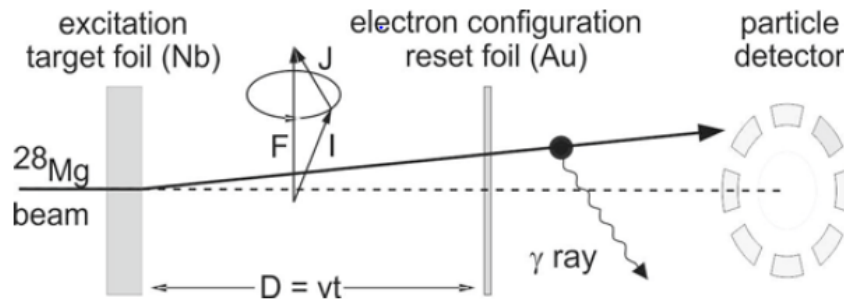


**Figure 2:** Illustration of the experimental method, showing the coupling of the nuclear and atomic spins after the Nb foil and its reset, after impinging on the reset foil. The gamma radiation pattern is detected by the MINIBALL array. The H-like ions experience the hyperfine interaction for a time depending on the distance between the target and the reset foil [5].

While the nuclear spin is periodically reduced and restored during the flight, the angular distribution pattern experiences damped oscillations, with the rate of damping depending on the lifetime of the nuclear state. The H-like ions will then impinge on a thin “reset” foil, which simply restores the electron configuration. Thus, by varying the distance of the Nb foil and the reset foil, an oscillatory pattern can be observed in the angular distribution of the emitted gamma rays, and consequently the frequency of the precession can be determined.

In order to analyze the data, time-dependent angular correlations have to be evaluated and ordered according to the amplitude of the oscillations, and whether the  $\gamma$  ray intensity should initially increase,  $W_i^\uparrow(T)$ , or decrease,  $W_i^\downarrow(T)$ , with time. Ratios of the coincidence  $\gamma$  ray intensity corresponding to  $W^\uparrow/W^\downarrow$  were formed in order, beginning with the pairing of the case showing strongest increase with the case of strongest decrease. These ratios were then formed into a geometric average:

$$R(T) = \left( \prod_{i=1}^n \frac{W_i^\uparrow(T)}{W_i^\downarrow(T)} \right)^{1/n}$$

where  $n$  is the number of  $W^\uparrow/W^\downarrow$  ratios included. Once the theoretical values of  $R(T)$  have been determined, simulated experimental values can be generated by randomly shifting the values within a Gaussian distribution whose width is determined by a chosen number of counts.

Ions that decay before reaching the reset foil are referred to as “fast”, while ions that decay after are referred to as “slow”. The TDRIV technique does not require that the  $\gamma$  rays emitted from the fast and slow ions should be separated in the observed energy spectrum [5].

## EXPERIMENTAL SETUP

The experiment took place at the ISOLDE facility. The  $^{28}\text{Mg}$  beam was post accelerated by REX-ISOLDE. The beam intensity at the MINIBALL target was about  $10^5$  pps. The subsequent  $\gamma$  decay pattern emitted due to the de-excitation of the first  $2^+$  state in  $^{28}\text{Mg}$  was detected by the MINIBALL spectrometer [6], positioned at angles close to  $\theta=90^\circ$  in order to

increase the sensitivity of the technique. The MINIBALL array consists of 8 triple-cluster, 6-fold segmented detectors for detecting the  $\gamma$  decay of the reaction products.

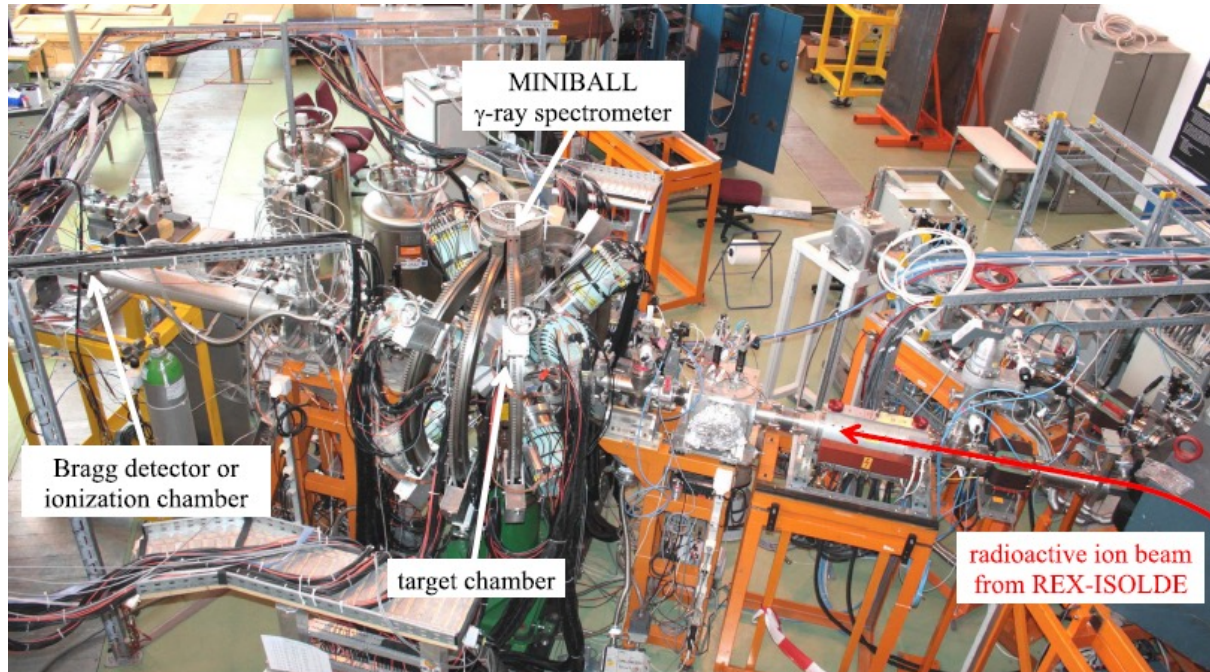


**Figure 3:** The experimental setup used for the IS628 experiment. The beam coming from REX-ISOLDE was directed in the MINIBALL array [4].

The MINIBALL DSSD CD detector has been used to detect the scattered beam particles. Particles were considered in the range  $20^\circ \leq \theta \leq 40^\circ$ , allowing to keep the safe Coulex process and thus calculate the particle- $\gamma$  angular correlations from first principles. The high granularity of both the Ge and CD detectors allow choosing the most sensitive combination for obtaining the highest amplitude of the R(T) function, where  $T = \text{flight time} = \text{distance}/\text{velocity}$ .

### TEST MEASUREMENT WITH THE $^{22}\text{Ne}$ BEAM - PRELIMINARY ANALYSIS

An important point for decreasing the uncertainty of the measurement was a test run, performed with a  $^{22}\text{Ne}$  beam, post-accelerated by the REX linac. By performing the test measurement with  $^{22}\text{Ne}$  under the same conditions as the  $^{28}\text{Mg}$  beam, it was possible to test the entire system with a well known probe. Furthermore, it will make possible the determination of the plunger distances sufficient precision, and thus decrease the uncertainty of the radioactive beam measurement. The excitation energy of the  $2_1^+$  state of  $^{22}\text{Ne}$ , its lifetime, and excitation probability are most suitable for a TDRIV measurement [7]. The  $^{22}\text{Ne}$  beam was provided by EBIS rest gas and did not require any proton beam nor the use of any of the separators.

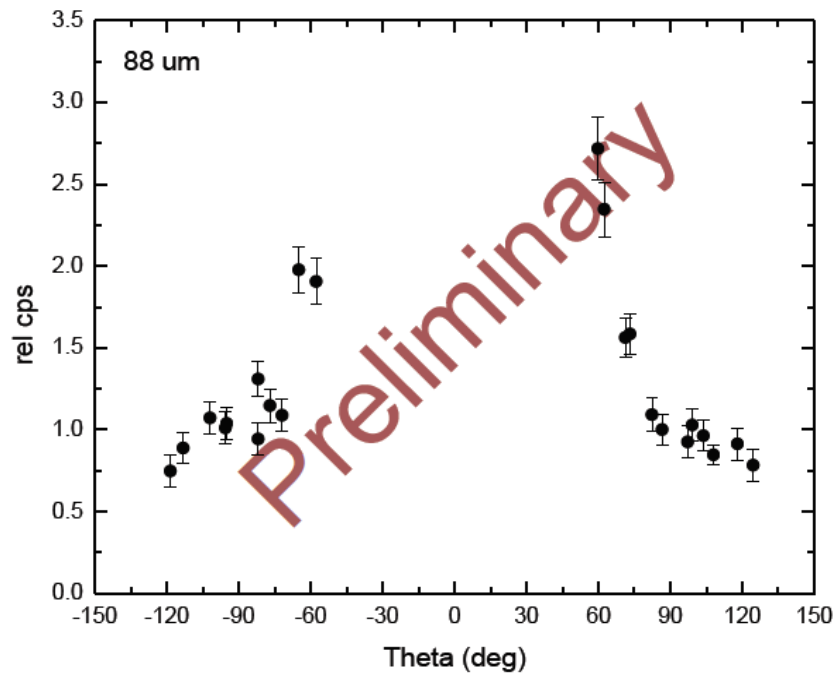


**Figure 4:** Perturbed angular distribution of the radiation emitted from the transition  $2_1^+ \rightarrow 0^+$  of  $^{22}\text{Ne}$ . The plunger target–reset foil distance is set here at 88  $\mu\text{m}$ .

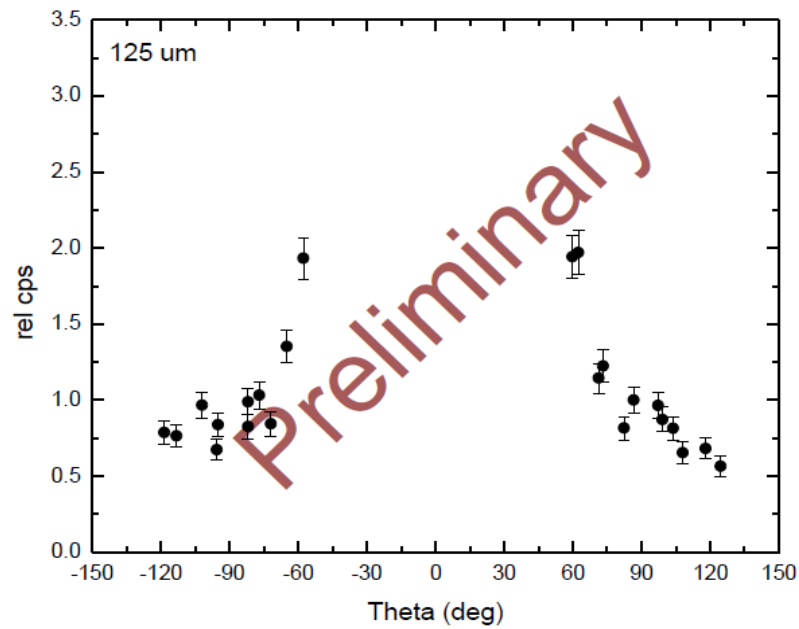


**Figure 5:** Perturbed angular distribution of the radiation emitted from the transition  $2_1^+ \rightarrow 0^+$  of  $^{22}\text{Ne}$ . The plunger target–reset foil distance is set here at 125  $\mu\text{m}$ .

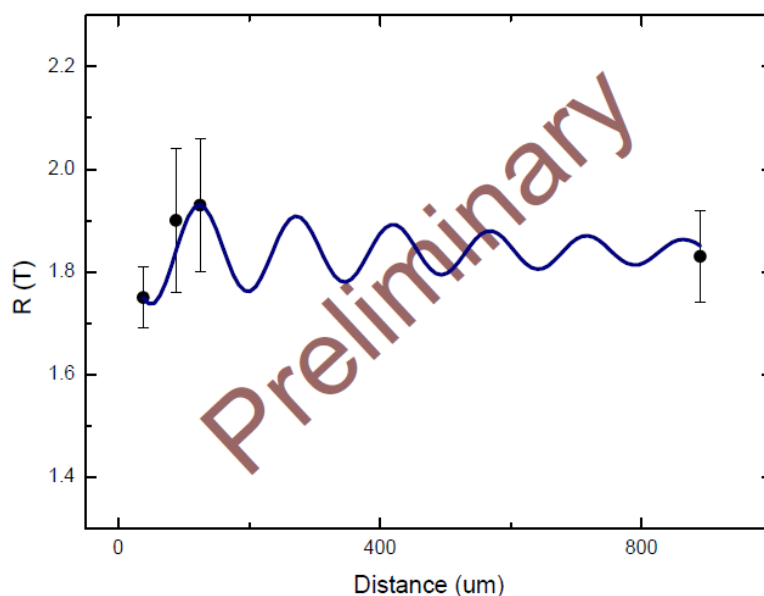


**Figure 6:** Ratio of counts as a function of the target–reset foil distance. Four distances are included: 38, 88, 125 and 890  $\mu\text{m}$ .

In Figures 4 and 5, two perturbed angular distributions of the  $\gamma$  rays emitted from the transition  $2_1^+ \rightarrow 0^+$  of  $^{22}\text{Ne}$ . These distributions were deduced from  $\gamma$  singles spectra and correspond to a plunger target–reset foil distance of 88  $\mu\text{m}$  and 125  $\mu\text{m}$ , respectively. All uncertainties are statistical, arising from photopeak integrations.

The dependence of the  $\gamma$  intensity at a certain angle as a function of the target–reset foil distance has also been preliminarily analyzed. The intensity of the radiation at  $\theta = 57^\circ$  is shown in Fig. 6, plotted for four target–reset foil distances. Although only a small portion of data has been analyzed so far, the behavior of the radiation intensity as a function of the plunger distance is showing the damped oscillatory pattern, as previously mentioned. The frequency of these oscillations will be proportional to the  $g$  factor of  $^{22}\text{Ne}$ . Using this as a known parameter, the plunger distances can now be precisely determined.

## CONCLUSION AND FUTURE DIRECTIONS

Analysis is currently on the works in order to determine the  $g$  factor of the first  $2^+$  state of  $^{28}\text{Mg}$  with sufficient precision. As a next step, the measurement of all angular distributions is essential to deduce the oscillatory pattern shown in Fig. 6. This will produce the precession frequency, and subsequently to the  $g$  factor.

The same procedure is currently being carried out for the test case of  $^{22}\text{Ne}$ . The  $g$  factor in this case is well known and this information will enable us to determine the target–reset foil distances with sufficient precision. Having deduced these distances, they will then be used as input for the determination of the  $g$  factor of  $^{28}\text{Mg}$ , leading to a decrease in the overall uncertainty of the measurement.

## ACKNOWLEDGEMENTS

AK acknowledges support from the HFRI–EΛIΔEK, No 694. Partial support from EU/ENSAR2 is also acknowledged.

## References

- [1] B.A. Brown and W.A. Richter, *Phys. Rev. C* **74**, 034315 (2006)
- [2] W.A. Richter, S. Mkhize and B.A. Brown, *Phys. Rev. C* **78**, 064302 (2008)
- [3] A. Kusoglu *et al.*, *Phys. Rev. Lett.* **114**, 062501 (2015)
- [4] P.A. Butler *et al.*, *J. Phys. G* **44**, 044012 (2017)
- [5] A.E. Stuchbery *et al.*, *Phys. Rev. C* **71**, 047302 (2005)
- [6] N. Warr *et al.*, *Eur. Phys. J. A* **49**, 40 (2013)
- [7] R.E. Horstmann *et al.*, *Nucl. Phys. A* **275**, 237 (1977)